Polymer Journal (2013) 45, 1027–1032

www.nature.com/pj

ORIGINAL ARTICLE

Nanoscale heterogeneous structure of polyacrylonitrile-co-butadiene with different molecular mobilities analyzed by spin–spin relaxation time

Hiroaki Ono[1], Hirotada Fujiwara[2] and Shin Nishimura[3]

To identify components with different spin–spin relaxation times, T_2, in the solid-echo pulse proton nuclear magnetic resonance (^{1}H-NMR) spectra of crude acrylonitrile (AN)–butadiene rubbers (NBRs) with five different AN contents, we tried to understand the inhomogeneity in the crude NBRs in terms of their microstructures and molecular mobilities. The results of small-angle X-ray scattering, differential scanning calorimetry and dynamic mechanical analysis showed that crude NBRs have a single-phase and homogeneous morphology on the nanoscale. The microstructure of the crude NBRs shows alternately copolymerized AN–butadiene (BU) and BU block sequences, as indicated by ^{1}H-NMR spectra. The T_2 of the crude NBRs revealed three components with different molecular mobilities, even in homogeneous samples. The content of the highest-mobility component with T_{2l} is negligible. Judging from the AN content dependence of the ^{1}H ratio of these components, the low-mobility component with T_{2s} and high-mobility component with T_{2m} were assigned to the alternately copolymerized AN–BU sequences and BU block sequences, respectively.
Polymer Journal (2013) **45,** 1027–1032; doi:10.1038/pj.2013.37; published online 10 April 2013

Keywords: molecular mobility; NBR; pulsed NMR; rubber; spin–spin relaxation time

INTRODUCTION

Synthetic rubber materials are widely used as sealing materials for various fluids. Rubber materials are designed in terms of the properties of target fluids for seals. For example, in the case of seals for gasoline, polar rubber should be used. In the case of gas seals, the transport of gas through sealing materials should be taken into account. From the perspective of the molecular design of rubbers as sealing materials, the clarification of the relationship between the structure of the rubbers and gas permeation phenomena, the effect of gas on the structure of the rubbers and the physical properties of the rubbers have become increasingly important. The molecular mobility of rubber molecules is one of the most important parameters to consider in designing suitable materials for rubber seals. There are several reports on the molecular mobility of rubber composites evaluated from the spin–spin relaxation time (T_2) of protons (^{1}H) in rubber molecules determined by free induction decay (FID) signals from pulsed proton nuclear magnetic resonance (pulsed ^{1}H-NMR) measurements.[1–4] Several methods for the evaluation of T_2 with different pulse sequences are available. The solid-echo pulse sequence method can evaluate relatively short T_2 [5]. Solid-echo pulse ^{1}H-NMR is widely used to analyze the crystallinity of polymer materials[6]. Information regarding the inhomogeneous structure of the bulk state of polymers can also be obtained using solid-echo pulse ^{1}H-NMR as the difference in T_2 for the components of the inhomogeneous state. Solid-echo pulse ^{1}H-NMR analysis can be used to understand the effect of pulsing on the permeation of fluids through sealing rubber materials. The time course of T_2 can be measured because of the short data acquisition time for FID signals. We have already reported on the solid-echo pulse ^{1}H-NMR analysis of the time course of T_2 for vulcanized acrylonitrile (AN)–butadiene rubber (NBR) composites, which are typical rubbers used for hydrogen gas sealing, after high-pressure hydrogen exposure to understand the effect of hydrogen on molecular mobility. We identified more than two components with different T_2 values in crude NBR using solid-echo pulse ^{1}H-NMR FID signals, and those T_2 values and the ^{1}H ratio of each T_2 value were determined to depend on the AN content of NBR. To understand the transport phenomena of hydrogen through sealing rubber materials according to the mobility of the molecular chains, each component of vulcanized NBR with a distinct T_2 value should be assigned by taking into account the inhomogeneous structure of crude rubber. Fukumori *et al.*[7] reported the solid-echo pulse ^{1}H-NMR analysis of vulcanized NBR. They found two components with different T_2 values, a short T_2 and a long T_2, which could be assigned to the rubber chains around crosslinks and the chains between crosslinks, respectively.

[1]Department of Hydrogen Energy Systems, Graduate School of Engineering, Kyushu University, Fukuoka, Japan; [2]The Research Center for Hydrogen Industrial Use and Storage, National Institute of Advanced Industrial Science and Technology, Fukuoka, Japan and [3]Department of Mechanical Engineering, Faculty of Engineering, Kyushu University, Fukuoka, Japan
Correspondence: Professor S Nishimura, Department of Mechanical Engineering, Faculty of Engineering, Kyushu University, 744 Motooka, Nishi-ku, Fukuoka 819-0395, Japan.
E-mail: nishimura.shin.691@m.kyushu-u.ac.jp
Received 30 October 2012; revised 16 January 2013; accepted 20 January 2013; published online 10 April 2013

However, there are no reports on the concrete assignment of these signals, even for crude rubber materials. NBR is generally polymerized by emulsion polymerization as a random copolymer. Although almost all random copolymers show homogeneous morphology, it has been reported that some random copolymers show an inhomogeneous phase structure.[8,9] In the case of NBRs, the existence of phase-separated structures was suggested by the spin–lattice relaxation time ($T_{1\rho}$) analysis of CH_2 via the ^{13}C-NMR inversion recovery method.[10] According to these reports, the inhomogeneity was caused by an intramolecular inhomogeneous structure composed of segments with different monomer sequences and by large differences in the segmental interaction parameters. However, there are no reports on the relationship between the inhomogeneity in the molecular mobility and in the microstructure of copolymer chains. The inhomogeneity of crude NBRs can be confirmed by small-angle X-ray scattering (SAXS), differential scanning calorimetry (DSC) and dynamic mechanical analysis (DMA). In this study, to identify definitively a wide range of T_2 components from solid-echo pulse ^{1}H-NMR FID signals of crude NBRs, we tried to understand the inhomogeneity in crude NBRs in terms of their microstructures and molecular mobilities.

EXPERIMENTAL PROCEDURE

Crude NBRs with five different AN contents, low (L), middle (M), middle high (MH), high (H) and very high (VH), were obtained from the Zeon Corporation (Tokyo, Japan): Nipol DN401 (L, AN: 18%), Nipol 1043 (M, AN: 29%), Nipol 1042 (MH, AN: 33.5%), Nipol 1041 (H, AN: 40.5%) and Nipol DN003(VH, AN: 50%), respectively. The details of the samples are shown in Table 1. The AN contents described above were specified by the supplier. M_e, the molecular weight between entanglements, was estimated from the storage elastic modulus at 30 °C analyzed by DMA. All measurement samples were used without any further purification.

Solution ^{1}H-NMR (ECP-400 400 MHz; JEOL Ltd., Akishima, Japan) measurements of the crude NBRs were performed in chloroform-d. The measurement of the crude NBRs was conducted with a single-pulse sequence (pulse width: 23 ms; pulse power: 34 W; acquisition time: 6.87 ms; observation center: 5.0 p.p.m.; sweep width: 20 p.p.m.; scan repetition: 64 times) using a ϕ5-mm solution probe.

DSC (DSC 204 HP; Netzsch, Selb, Germany) was performed from −100 to 150 °C in air. The heating rate was 10 °C min^{-1}.

DMA (itk DVA-225; IT Keisokuseigyo, Osaka, Japan) was performed from −100 to 150 °C. The shear stress frequency was 2.5 Hz. M_e was calculated by using equation (1):

$$M_e = \frac{\rho RT}{G`} \quad (1)$$

where ρ is the sample density, R is the universal gas constant, T is temperature and G' is the storage elastic modulus. G' values at 30 °C were used; thus, T was 303.15.

SAXS (Nanostar; Bruker AXS, Karlsruhe, Germany) was performed on crude NBR films measuring 5 mm in thickness. The wavelength of the Cu Kα X-ray beam was 0.154 nm, and the camera length (sample detector) was 1053 mm. Scattering patterns were collected with a two-dimensional detector (Vantec-Hi Star; Bruker AXS).

The solid-echo ($90^\circ_x - \tau - 90^\circ_y$) FID signals of the samples were analyzed by using pulsed ^{1}H-NMR (minispec mq20, 20 MHz; Bruker BioSpin, Karlsruhe, Germany) at 30 °C. Samples (ϕ10 mm × 10 mm) were placed in ϕ10 mm Pyrex tubes. The T_2 values and ^{1}H ratios of the T_2 values were calculated from the obtained FID signals by the converged equation (2) using the least-squares method,

$$\mathrm{Int} = \sum_{i=1}^{N} A_i \exp\left(-\left(\frac{1}{\alpha_i}\right)\left(\frac{t}{T_{2i}}\right)^{\alpha_i}\right) + c \quad (2)$$

where A_i is the intensity at time 0, t is time, T_{2i} is the T_2 value of ith component and α_i is the FID signal shape constant. The ^{1}H ratios of T_{2i} were evaluated using M_i, as shown in equation (3):

$$M_i = A_i / \sum_i A_i \quad (3)$$

RESULTS AND DISCUSSION

Monomer sequence distribution of crude NBRs

To determine the monomer sequence distribution of the crude NBRs, the solution ^{1}H-NMR spectra of these samples were measured. Figure 1 shows the spectrum of MH. The protons of methine (C*H*) at the center of the triad were observed in the regions of 2.5–2.9 and 5.2–5.7 p.p.m. The signals of C*H* were divided into five regions: 5.5–5.67, 2.85, 2.58, 2.85 and 5.2–5.43 p.p.m., which were assigned to the triads of NBR, ABA, BAA, BAB, BBA and BBB, respectively,[11] where A is an AN unit and B is a butadiene (BU) unit. The C*H* of AAA, which were observed at 3.1 p.p.m.[12] in polyacrylonitrile, were not detected in the spectra of the crude NBRs. The average contents of AN, BU and triad distributions were calculated from the area of these signals.

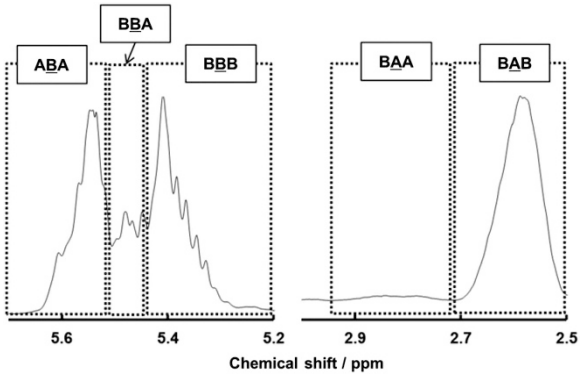

Figure 1 Proton nuclear magnetic resonance (^{1}H-NMR) spectrum of crude acrylonitrile–butadiene rubber (NBR) (MH) in chloroform-d.

Table 1 Sample information

Sample		*Product*	*AN (wt%)*	ρ *(g cm^{-3})*	*MV*	M_e *(kg mol^{-1})*
L		DN401	18.0	0.94	77.5	2.0
M		1043	29.0	0.97	77.5	2.2
MH	Nipol	1042	33.5	0.98	77.5	1.8
V		1041	40.5	1.00	82.5	2.5
VH		DN003	50.0	1.02	77.5	2.2

Abbreviations: AN, official value of acrylonitrile content of crude NBRs; ρ, official value of density of crude NBRs; MV, official value of Mooney viscosity; M_e, molecular weight between entanglements from storage elastic modulus at 30 °C analyzed by dynamic mechanical analysis; NBR, acrylonitrile–butadiene rubber.

Table 2 Average chemical composition and triad distributions of crude NBR

	Morlar ratio (%)							
Samples	*AN*	*BU*	*AAA*	*BAB*	*BAA*	*BBB*	*BBA*	*ABA*
L	21	79	0	21	0	48	13	19
M	30	70	0	30	0	29	13	28
MH	35	65	0	34	1	28	12	26
H	41	59	0	39	2	16	10	33
VH	49	51	0	38	10	5	5	42

The average chemical composition and triad distribution of the crude NBRs determined by solution ^{1}H-NMR are shown in Table 2.

The contents of ABA and BAB increased with the AN content. The contents of BBA and BBB clearly decreased with increasing AN content. These results suggest that in crude NBRs, AN units prefer alternate or random copolymerization with BU units; however, BU units prefer the formation of BU blocks.

The average sequence lengths of AN (L_n[AN]) and BU (L_n[BU]) in each crude NBR were calculated using equations (4) and (5),[13]

$$L_n[\mathrm{AN}] = (F_{\mathrm{BAB}} + F_{\mathrm{BAA}} + F_{\mathrm{AAA}})/(F_{\mathrm{BAB}} + \frac{F_{\mathrm{BAA}}}{2}) \quad (4)$$

$$L_n[\mathrm{BU}] = (F_{\mathrm{ABA}} + F_{\mathrm{BBA}} + F_{\mathrm{BBB}})/(F_{\mathrm{ABA}} + \frac{F_{\mathrm{BBA}}}{2}) \quad (5)$$

where F_{AAA}, F_{BAB}, F_{BAA}, F_{BBB}, F_{BBA} and F_{ABA} are the molar fractions of the triads. The relationship between the AN content and L_n[AN], L_n[BU] is illustrated in Figure 2. As shown in Figure 2, L_n[BU] decreased proportionally with the increase in the AN content. In contrast, L_n[AN] remained constant. The relationship between the mole fraction of BU units in the polymer (F_{BU}) and the mole fraction of feedstock AN monomer (f_{AN}) was calculated using equation (6),[14]

$$F_{\mathrm{BU}} = \frac{r_{\mathrm{BU}} f_{\mathrm{BU}^2} + f_{\mathrm{BU}} f_{\mathrm{AN}}}{r_{\mathrm{BU}} f_{\mathrm{BU}}^2 + 2 + r_{\mathrm{AN}} f_{\mathrm{AN}^2}} \quad (6)$$

where f_{AN} and f_{BU} are the mole fractions of feedstock AN and BU monomers, respectively, and $r_{\mathrm{AN}}(=0.03)$ and $r_{\mathrm{BU}}(=0.2)$ are the AN and BU monomer reactivity ratios, respectively.[15] The calculated results are shown in Figure 3. According to this figure, in the region of $f_{\mathrm{AN}} = 0.2$–0.8, f_{BU} was nearly 0.5. During the early stages of copolymerization, an AN–BU alternate copolymer was produced, and during the later stages, BU blocks were produced by the remaining BU monomer.

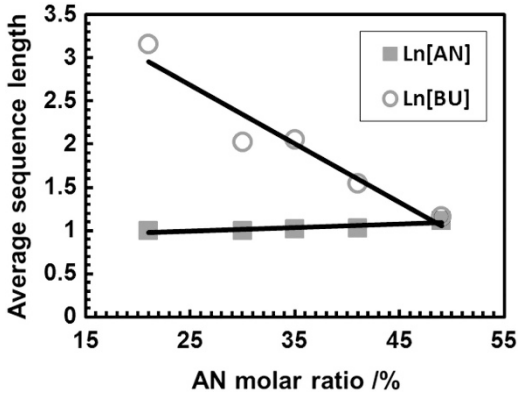

Figure 2 Relationship between acrylonitrile (AN) content and average sequence length of AN (L_n[AN]) and butadiene (BU) (L_n[BU]). A full color version of this figure is available at *Polymer Journal* online.

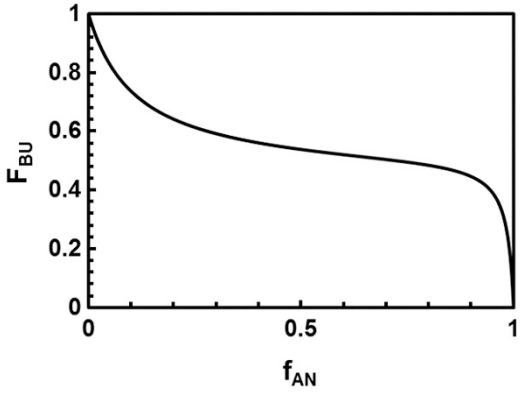

Figure 3 Relationship between molar fraction of butadiene (BU) in polymer chains and molar fraction of feedstock acrylonitrile (AN) monomer.

According to these results, crude NBR chains consist of two components, a BU block sequence and an alternately copolymerized AN–BU sequence, at low and high AN contents components, respectively.

Morphological analysis of crude NBRs by SAXS

We tried to estimate the size of aggregated AN–BU chains by using SAXS, and the obtained scattering profile was analyzed by Fankuchen's method.[16] For monodisperse aggregates with a radius of gyration R, the SAXS intensity can be described by Guinier's method using equation (7),

$$I(q) = I(0)\exp(-\frac{q^2 R_{\mathrm{g}}^2}{3}) \quad (7)$$

where $I(q)$ is the SAXS intensity, $I(0)$ is the intensity of $q=0$, q is the scattering vector and R_{g} is the radius of gyration. However, for polydisperse aggregates with radii of gyration R_{g}, the distribution of R_{g} can be calculated by Fankuchen's method using equation (8):

$$I(q) = \sum_i I(0)_i \exp(-\frac{q^2 R_{gi}^2}{3}) \quad (8)$$

Equation (8) is a summation of equation (7). Thus, equation (8) can be described by a double logarithm as follows:

$$\ln \mathrm{I(q)} = \sum_i \ln I(0)_i \exp(-\frac{q^2 R_{gi}^2}{3}) \quad (9)$$

Thus, according to equation (7), R_{gi} can be calculated from the slope of the plot of $\ln(I(q))$ vs q^2, the so-called Guinier plot. The relationship between the slope (S_i) and R_{gi} and the relationship between R_{gi} and the particle radius (R_i) are described by equations (10) and (11), respectively. The mass ratio of components with R_{gi} can be calculated by equation (12):[17]

$$S_i = -\frac{R_{gi}^2}{3} \quad (10)$$

$$R_i = \sqrt{\frac{5}{3}} R_{gi} \quad (11)$$

$$W(R_{gi}) = \frac{I(0)_i}{R_{gi}^3} / \sum_i \frac{I(0)_i}{R_{gi}^3} \quad (12)$$

Guinier plots of the crude NBRs are shown in Figure 4, and sample slopes of the Guinier plots are shown in Figure 5. The estimated values of R_i and $W(R_i)$ are shown in Table 3. Three slopes were obtained from the Guinier plots. As shown in Table 3, the obtained R_i were 0.13–0.37, 3.62–5.21 and 11.7–14.6 nm. The two larger domains exhibited quite small mass ratios. According to the results of SAXS, the crude NBRs were regarded as having a single-domain morphology, that is, nanodomain aggregates with $R_i = 0.13$–0.37 nm. In other words, the crude NBRs exhibited a homogeneous morphology on the nanoscale.

Thermal analysis for glass transition temperature

From the results of morphological analysis, it was concluded that the crude NBRs were single phase. To confirm the uniformity of the

materials, DSC and DMA measurements were performed on crude NBR samples to evaluate their glass transition temperatures (T_g).

Figure 6 shows the DSC curves of the crude NBRs. The curves show two endothermic peaks for all samples. The T_g of each sample was determined as the downward peak of the first-order derivative of the corresponding DSC curve. The main endothermic peak temperatures below 0 °C were designated as the T_g values of the crude NBRs.

Chandler *et al.*[18] reported that the results of differential thermal analyses for crude NBRs with <36% AN showed two T_g values below 0 °C because of the existence of a phase-separated structure in the samples. [18] In the case of emulsion-polymerized NBR, the monomer sequence distribution was dominated by the polymerization temperature and conversion rate.[19] However, our DSC results for crude NBRs show only one T_g.

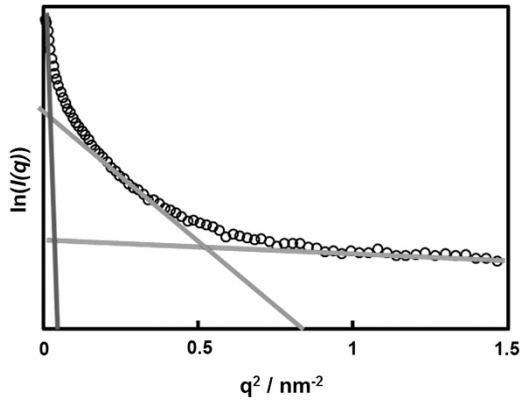

Figure 4 Guinier plot and MH slope. A full color version of this figure is available at *Polymer Journal* online.

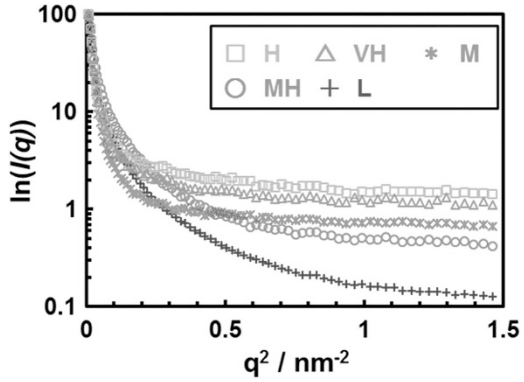

Figure 5 Guinier plot of crude acrylonitrile–butadiene rubbers (NBRs). A full color version of this figure is available at *Polymer Journal* online.

Figure 7 shows the temperature dependence of tan δ measured by DMA for crude NBR samples. T_g was determined as the peak temperature of tan δ. The tan δ values showed a single peak in all samples. These peak temperatures were designated the T_g values. T_g increased as the AN content increased. Thus, only one T_g was observed in not only the DSC profiles but also the DMA profiles.

Judging from our SAXS, DSC and DMA results, the crude NBRs used in this study showed a single-phase and homogeneous morphology.

Pulsed ^{1}H-NMR analysis of crude NBRs

The observed FID signals and fitted FIDs for crude NBRs at 30 °C are shown in Figure 8. The FID signals obtained were fitted by

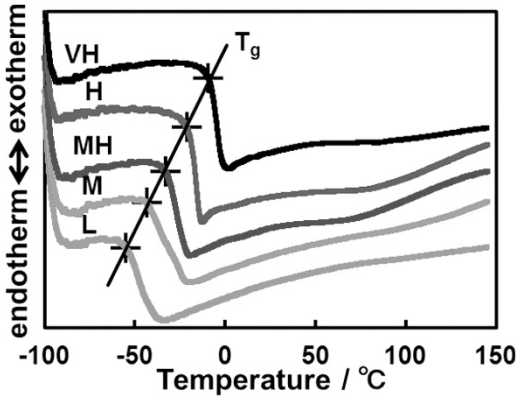

Figure 6 Differential scanning calorimetry (DSC) curves of crude acrylonitrile–butadiene rubbers (NBRs). A full color version of this figure is available at *Polymer Journal* online.

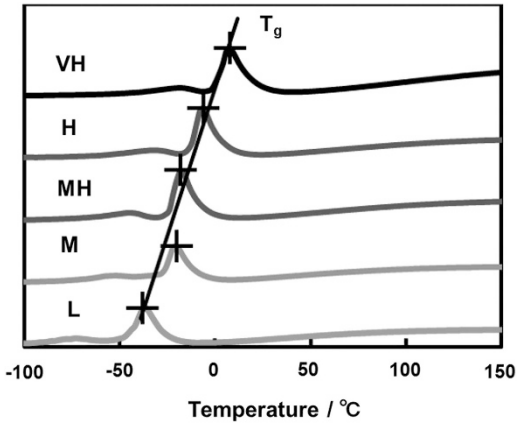

Figure 7 Tan δ of crude acrylonitrile–butadiene rubbers (NBRs). A full color version of this figure is available at *Polymer Journal* online.

Table 3 Radius of domain (R_i) and weight fraction of domain with R_i of crude NBRs

L		*M*		*MH*		*H*		*VH*	
R_i *(nm)*	$W(R_i)$	R_i *(nm)*	$W(R_i)$	R_i *(nm)*	$W(R_i)$	R_i *(nm)*	$W(R_i)$	R_i *(nm)*	$W(R_i)$
0.37	1.00	0.23	1.00	0.26	1.00	0.13	1.00	0.16	1.00
3.84	4.69×10^{-4}	5.21	1.34×10^{-5}	4.46	8.86×10^{-5}	3.62	4.86×10^{-6}	4.40	6.41×10^{-6}
11.8	1.09×10^{-5}	11.82	3.17×10^{-6}	14.6	1.48×10^{-6}	11.9	4.95×10^{-7}	11.7	1.03×10^{-6}

Abbreviations: NBR, acrylonitrile butadiene rubber; R_i, radius of domain; $W(R_i)$, weight fraction of domain with R_i.

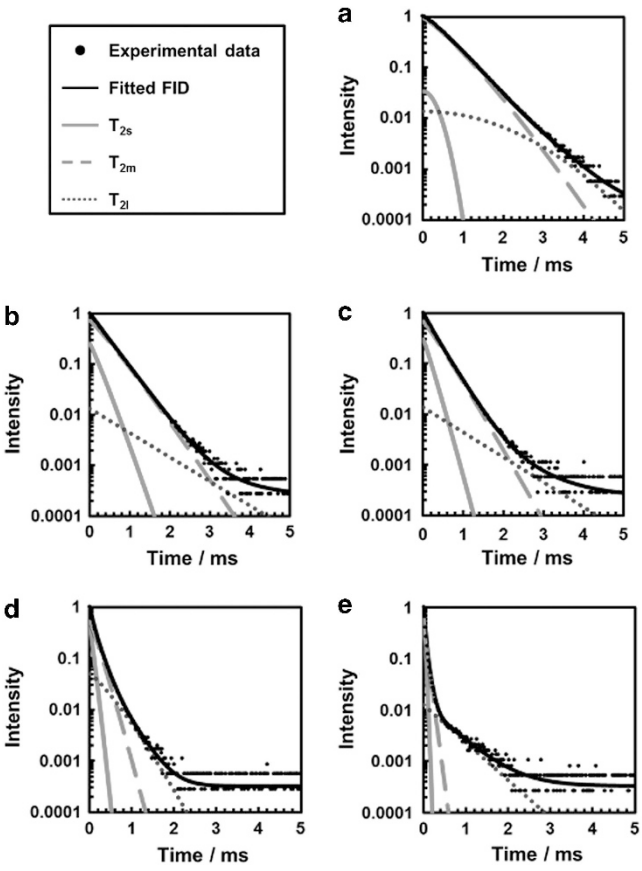

Figure 8 Free induction decay (FID) signals of pulsed proton nuclear magnetic resonance (^{1}H-NMR) spectra with fitting results for crude (NBRs): (**a**) L, (**b**) M, (**c**) MH, (**d**) H and (**e**) VH. A full color version of this figure is available at *Polymer Journal* online.

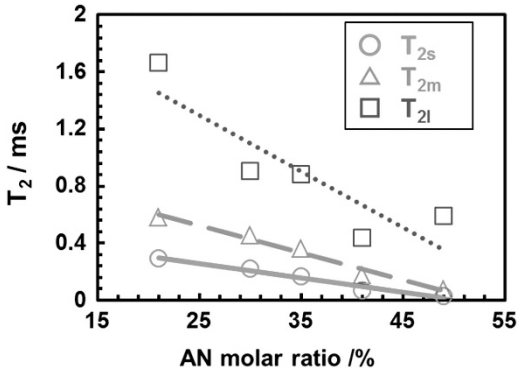

Figure 9 The relationship between acrylonitrile (AN) content and T_2. A full color version of this figure is available at *Polymer Journal* online.

equation (1) using the least-squares method. A_i, N, α_i and T_{2i} in equation (1) were treated as fitting parameters. As indicated by the fitting results, the number of components N for each crude NBR was 3. The residual sums of the squares of the fitting results were below 10^{-4}. The FID signals of all of the samples could be separated into three T_2 components denoted T_{2s}, T_{2m} and T_{2l}. The relationship between AN content and T_2 analyzed by pulsed ^{1}H-NMR is illustrated in Figure 9. T_{2s}, T_{2m} and T_{2l} decreased proportionally with increasing AN content. Figure 10 shows the amount of each component as the ^{1}H ratio. As shown in Figure 10, the ^{1}H ratio of the component with

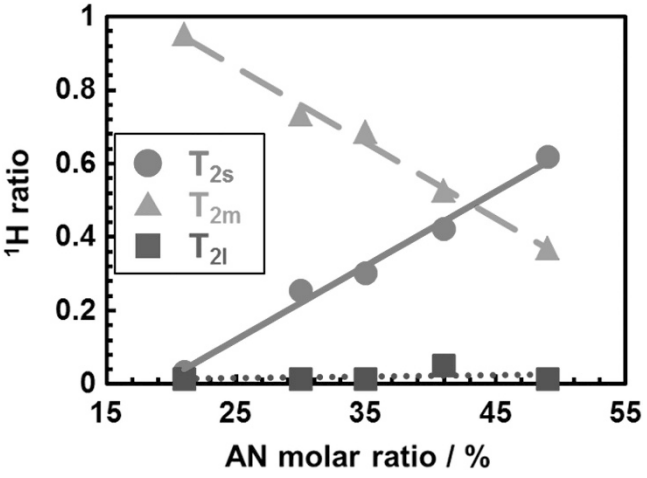

Figure 10 The relationship between acrylonitrile (AN) content and ^{1}H ratio with T_2. A full color version of this figure is available at *Polymer Journal* online.

T_{2s} increased and that with T_{2m} decreased as the AN content increased. The ^{1}H ratio with T_{2l} was quite small and remained constant. These results indicate that there were two components with different molecular mobilities in the crude NBRs. The mobility of each component depends on the AN content of the component. The number of polar monomer units increases with AN content. The increase in the number of polar monomer units causes a decrease in molecular mobility. Kwak and Kim[10] reported the observation of local phase separation into sea–island structures in crude NBRs from the analysis of the spin–lattice relaxation time $T_{1\rho}$ of CH_2. Faghihi *et al.*[8] reported that random copolymers of butyl acrylate and methyl methacrylate showed nanophase segregation according to DMA, DSC and ^{13}C-NMR spin diffusion experiments. Kipper *et al.*[9] reported that random copolymers of 1,6-bis(*p*-carboxyphenoxy)hexane and sebacic acid undergo microphase separation because of large differences in the segment–segment interaction parameters. In this study, the crude NBRs did not show a phase separation structure. Two components with different molecular mobilities were observed in the crude NBRs.

Assignment of components with T_{2s} and T_{2m} of crude NBRs

According to the results of solution ^{1}H-NMR, crude NBR chains consist of two components, a BU block sequence and an alternately copolymerized AN–BU sequence, at low and high AN contents, respectively. According to the results of SAXS, the crude NBRs showed a single-domain morphology, that is, the aggregation of nanodomains. The DSC curves and tan δ peaks of the crude NBRs show one T_g. The crude NBRs were determined to exhibit homogeneous morphology on the nanoscale. The spin–spin relaxation time, T_2, determined by pulsed ^{1}H-NMR for crude NBRs showed mainly two components with different molecular mobilities, even in homogeneous samples. The ^{1}H ratio of T_{2s} increased and that of T_{2m} decreased with increasing AN content. As shown in Table 1, the molecular weights between entanglements, M_e, for all samples were all close to 2.0 kg mol^{-1}, despite the differences in the AN content among the samples. Judging from the dependence of the ^{1}H ratio on the AN content, T_{2s} and T_{2m} were assigned to the alternately copolymerized AN–BU sequence, which is strongly constrained by intermolecular interactions between polar nitrile groups and BU block sequences, which are weakly constrained.

CONCLUSIONS

To understand the transport phenomena of hydrogen through sealing rubber materials by examining the mobility of their molecular chains, each component with a distinct T_2 in vulcanized NBR should be assigned by taking into account the inhomogeneous structure of crude rubber. In this study, to identify definitively a wide range of T_2 components from the solid-echo pulsed ^{1}H-NMR FID signals of crude NBRs, we tried to understand the inhomogeneity of the crude NBRs in terms of their monomer sequence distribution and molecular mobility. The crude NBRs show homogeneous morphology on the nanoscale; however, the spin–spin relaxation time, T_2, determined by pulsed ^{1}H-NMR for the crude NBRs showed three components with different molecular mobilities, even in homogeneous samples. The content of the highest-mobility component with T_{2l} was negligibly small. Judging from the dependence of the ^{1}H ratio on the AN content in these components, the low-mobility component with T_{2s} and the high-mobility component with T_{2m} were assigned to the alternately copolymerized AN–BU sequence and BU block sequence, respectively. The inhomogeneity of crude NBR may be attributed to its monomer sequence distribution.

ACKNOWLEDGEMENTS

This research has been supported by the New Energy and Industrial Technology Development Organization (NEDO) 'Fundamental Research Project on Advanced Hydrogen Science (2006–2012)'.

1 Borgia, G. C., Fantazzini, P., Ferrando, A. & Maddinelli, G. Characterisation of crosslinked elastomeric materials by ^{1}H NMR relaxation time distributions. *Magn. Reson. Imaging* **19,** 405–409 (2001).
2 Whittaker, A. K., Bremner, T. & Zelaya, F. O. The effect of field inhomogeneities and molecular diffusion on the NMR transverse relaxation behaviour of polymer melts. *Polymer* **36,** 2159–2164 (1995).
3 Garrido, L., Mark, J. E., Sun, C. C., Ackerman, J. L. & Chang, C. NMR characterization of elastomers reinforced with *in situ* precipitated silica. *Macromolecules* **24,** 4067–4072 (1991).
4 O'Brien, J., Cashell, E., Wardell, G. E. & McBrierty, V. J. An NMR investigation of the interaction between carbon black and *cis*-polybutadiene. *Macromolecules* **9,** 653–660 (1976).
5 Fukumori, K., Kurauchi, T. & Kamigaito, O. Pulsed NMR study of elastomeric block copolymer under deformation. *J. Appl. Polym. Sci.* **38,** 1313–1334 (1989).
6 Uehara, H., Yamanobe, T. & Komoto, T. Relationship between solid-state molecular motion and morphology for ultrahigh molecular weight polyethylene crystallized under different conditions. *Macromolecules* **33,** 4861–4870 (2000).
7 Fukumori, K., Norio Sato, N. & Kurauchi, T. Deformation behaviors of nitrile rubber vulcanizates as studied by pulsed NMR: effects of carbon black fillers. *Nippon Gomu Kyoukaishi* **61,** 561–566 (1988).
8 Faghihi, F., Mohammadi, N. & Hazendonk, P. Effect of restricted phase segregation and resultant nanostructural heterogeneity on glass transition of nonuniform acrylic random copolymers. *Macromolecules* **44,** 2154–2160 (2011).
9 Kipper, M. J., Hou, S. -S., Seifert, S., Thiyagarajan, P., Schmidt-Rohr, K. & Narasimhan, B. Nanoscale morphology of polyanhydride copolymers. *Macromolecules* **38,** 8468–8472 (2005).
10 Kwak, S. -Y. & Kim, S. Y. Microphase structures of polymers containing structural heterogeneity as probed by n.m.r. spin–lattice relaxation analysis. *Polymer* **39,** 4099–4105 (1998).
11 Anachkov, M. P., Stefanova, R. V. & Rakovsky, S. K. ^{1}H NMR study of monomer sequence distributions in some commercial acrylonitrile–butadiene copolymers. *Br. Polym. J.* **21,** 429–432 (1989).
12 Pai Verneker, V. R. & Shaha, B. On coloration of polyacrylonitrile: a nuclear magnetic resonance study. *Macromolecules* **19,** 1851–1856 (1986).
13 Matsuda, H., Asakura, T. & Miki, T. Triad sequence analysis of poly(ethylene/butylene terephthalate) copolymer using ^{1}H NMR. *Macromolecules* **35,** 4664–4668 (2002).
14 Hiemenz, P.C & Lodge, T. P. *Polymer Chemistry.* 2nd edn. Vol. 168 (CRC Press, New York, NY, USA, 2007).
15 Greenley, R.Z. in *Polymer Handbook.* 4th edn (eds. Brandrup, J., Immergut, E. H., Grulke, E. A., Abe, A. & Bloch, D. R.) Ch. 2, 203 (Wiley, New York, NY, USA, 1999).
16 Wang, X. -S., Kim, H. -K., Fujita, Y., Sudo, A., Nishida, H. & Endo, T. Relaxation and reinforcing effects of polyrotaxane in an epoxy resin matrix. *Macromolecules* **39,** 1046–1052 (2006).
17 Rigaku X-ray Research Laboratory *X-ray diffraction Handbook* 115–116 (Rigaku, Japan, 2000).
18 Chandler, L. A. & Collins, E. A. Multiple glass transitions in butadiene–acrylonitrile copolymers. *J. Appl. Polym. Sci.* **13,** 1585–1593 (1969).
19 Hashimoto, K. in *Rubber Industrial Handbook (The Society of Rubber Science and Technology* Ch. 2, 238The Society of Rubber Science and Technology, 1994).